Polar Cloud-Detection Algorithms for a Real-Time Analysis and Forecasting Model

Robert P. d'Entremont and Gary B. Gustafson
Satellite Meteorology Group
Atmospheric and Environmental Research, Inc. Lexington, MA

1 Introduction

This paper describes the new polar cloud-detection segment of the US Air Force Cloud Depiction and Forecast System (CDFS-II), which is run operationally at the Air Force Weather Agency at Offutt AFB, NE. Existing CDFS polar modules did not capitalize on the availability of AVHRR 1.6-μm data in daylight conditions, and were poorly suited to adapt to the extreme background conditions of snow and ice in the long polar night. We also have developed a temporal differencing technique with several channels of polar orbiter data, analogous to the geostationary technique described in d'Entremont and Gustafson (2003).

A list of the sensor channels used in our detection algorithms is found in Table 1 below. The primary imager data sources are the NOAA-TIROS AVHRR and DMSP Operational Linescan (OLS) systems. Our algorithms automatically adapt to the availability (or non-availability) of channels from each source.

Our work on this project is part of a long line of research in the area of polar cloud detection algorithms (see, for example, Liu et al., 2004; Shi et al., 2004; Spangenburg et al., 2002).

Table 1. List of sensor channel names used in this paper

Sensor Channel Name	Description	Generic Name
OLS–L	0.4 – 1.0 μm visible count	VIS
OLS–T	10.5 – 12.6 μm brightness temperature	TIR1
AVHRR-1	0.58 – 0.68 μm percent albedo	VIS
AVHRR-2	0.72 – 1.10 μm percent albedo	NIR
AVHRR-3a	1.58 – 1.64 μm percent albedo	SWIR
AVHRR-3b	3.55 – 3.93 μm brightness temperature	MWIR
AVHRR-4	10.3 –11.3 μm brightness temperature	TIR1
AVHRR-5	11.5 – 12.5 μm brightness temperature	TIR2

2 Snow/Ice Cover Background Test

The Snow/Ice background test identifies regions of snow and ice cover in an otherwise cloud-free polar scene. The test is designed to operate with either 1.6-μm SWIR albedo or 3.7-3.9 μm MWIR data to accommodate the AVHRR channel 3a/b switching (Figure 1 illustrates how the 3a/b switchover occurs over a few scan lines). Since both versions of the background test rely on a reflected signature they can only be applied during daylight conditions.

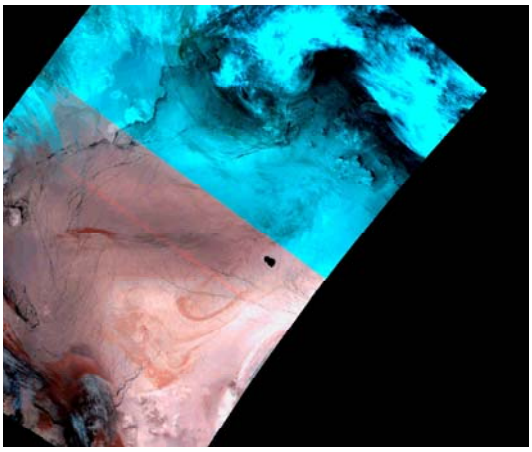

Figure 1. Composite MWIR-TIR image showing the switchover between AVHHR-3 channels 3a and 3b at the terminator

When SWIR data are available the test exploits the fact that the imaginary refractive index of ice is much higher at SWIR wavelengths than it is at near-IR and visible wavelengths. Radiative-transfer physics subsequently dictates that SWIR energy is absorbed strongly by snow and ice, while these surfaces reflect near-IR and visible light with greater efficiency. The primary snow detection discriminator is the magnitude of the Normalized Difference Snow Index (NDSI), defined as the ratio

$$NDSI = (SWIR - NIR) / (SWIR + NIR).$$

The range of this metric is $-1 \leq NDSI \leq 1$. As snow cover becomes more dense, SWIR absorption grows stronger while at the same time its near-IR reflection increases. This serves to make the numerator in the NDSI definition smaller (and negative) – thus as NDSI gets smaller, the likelihood of a pixel's containing snow or ice cover increases. Low water-droplet clouds reflect equally well in both bands and so NDSI is near zero. For this reason the NDSI and other metrics like it are often referred to as snow-cloud discriminators.

This test is designed primarily to detect snow and ice covers. It is possible that cirrus clouds, also composed of ice particles, will trip this test. However, only the highest-density ice masses will have the lowest NDSI values; careful selection of the NDSI threshold will screen out the optically thinner and much less dense cirrus. For reasons that are unclear, it is also possible for this test to flag open water pixels, even when the NDSI threshold is set very low. (The suspicion is that atmospheric scattering, albeit quite small in the near-IR and SWIR

bands, is nonetheless much stronger in the near-IR than it is in the SWIR, yielding a negative NDSI.) Accordingly, a final check on the absolute magnitude of the NIR reflectance observation is made to ensure the pixel's brightness is high enough to indicate snow or ice.

If no SWIR data are available then the MWIR reflectance is estimated by subtracting off the TIR1 brightness temperature from the MWIR observation. Clouds will generally result in a positive VIS/NIR – MWIR reflectance difference, snow/ice with a much smaller difference. To avoid confusion with ice-phase clouds a further constraint is added wherein the IR brightness temperature must be fairly close to the predicted clear-scene temperature.

NDSI has a built-in advantage in that it automatically cancels out a lot of the dependencies on the view and illumination geometries of the pixel being observed. For example, imagine that the NIR and SWIR reflectances have to be normalized to sun overhead. Dividing all NDSI quantities by $\cos\theta_{sat}$ is certainly possible, but these adjustment factors will cancel out in the NDSI calculation. This allows for NDSI to be computed and used with accuracy with all SWIR data from the moment the MWIR-to-SWIR switch is enabled near the terminator.

3 Obvious Bright Cloud Test for Polar Backgrounds

The obvious-bright cloud test compares near-IR channel data to an empirically defined 0.86-μm reflectance threshold. Any pixel whose near-IR reflectance is at or higher than this threshold is always considered cloud-filled. The primary cloud discriminator is the absolute magnitude of a cloud's bidirectional reflectance. Reflectance at near-IR wavelengths is a strong indicator of cloud extinction optical thickness but, to a much smaller degree, is also confounded by effective particle size. The test is designed primarily to detect clouds that are obviously bright, i.e., that have high extinction optical thicknesses.

However, polar backgrounds of ice and snow typically have little or no contrast with clouds in daytime conditions since they too reflect solar energy efficiently. False-cloud detection over snow and ice is mitigated through the use of a 1.6-μm SWIR snow/ice test: if the snow test classifies a previously obvious-bright pixel as snow/ice-filled, the obvious-bright test is turned off. This does not occur until the final cloud-mask decision is performed.

In the Polar Regions, near-IR data are used in place of the more traditional 0.63-μm visible data since adverse atmospheric scattering effects are considerably weaker. Although polar atmospheres are quite free of aerosols most of the time, the overall atmospheric

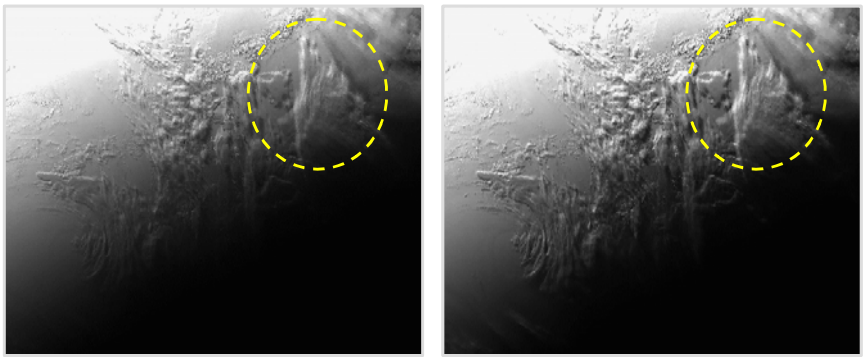

Figure 2. Comparison of visible (left) and near-IR (right) reflectance images near the wintertime terminator over the north pole in February. Note the increased cloud-feature contrast in the near-IR image

molecular scattering effects are quite strong because, with low solar elevation angles, the incident solar-photon paths are long - in turn increasing substantially the likelihood of a photon's interaction with at least one atmospheric molecule. With fewer visible photons reaching the satellite unaltered by the intervening atmosphere, the scene elements appear less clearly than when the sun is higher in the sky.

Atmospheric scattering loses its influence dramatically as wavelength increases from the visible portion toward the near-IR and SWIR portions of the electromagnetic spectrum. The net result is that scene-element contrasts improve quite noticeably, as is shown in Figure 2. This in turn allows for a more confident assessment, both visually and digitally, of the cloud scene itself. The near-IR sensor data are normalized by an empirical solar illumination adjustment function to account for variations across the terminator, as shown in Figure 3. In regions poleward of 70^{o}, the terminator can be found nearly year-round. This secant-adjustment table increases the amount of usable reflectances in regions where solar illumination is reduced near the terminator. Over both land and water backgrounds the secant-adjusted near-IR-channel albedo is compared to the empirically assigned clear/cloud boundary value obtained from the corresponding Polar-Region threshold database. If the reflectance is higher than the threshold then the pixel is classified as cloud filled.

It is possible that snow cover will be flagged improperly as cloud by this test. Accordingly the results of this test are turned off by the daytime snow-detection test if it succeeds in identifying obvious-bright pixels as snow- or ice-filled. However this step is not performed until the final cloud determination portion of the algorithm is performed.

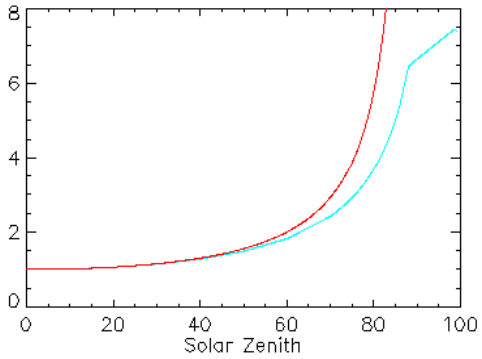

Figure 3. Comparison of secant function (red) and empirical solar illumination adjustment function (blue)

The threshold for the obvious-bright test over polar backgrounds is intentionally set so that all clouds will be detected, but oftentimes at the expense of flagging snow and ice as cloud too. The daytime snow-detection test results reset the snow/ice pixels as cloud-free. If the snow-test results are not available (i.e., if the SWIR data are not available), the obvious-bright test is not performed.

4 Obvious Cold Cloud Test for Polar Backgrounds

The obvious-cold cloud test compares 10.8-μm TIR1 brightness temperatures to an empirically defined brightness temperature threshold. Any pixel whose TIR1 infrared TOA brightness temperature is at or lower than this threshold is always considered cloud-filled. The primary cloud discriminator is the absolute magnitude of a cloud's effective blackbody temperature, which, for most optically thick clouds, is a strong indicator of their in-atmosphere vertical position. The lower the temperature the farther from the ground the remotely sensed object lies, thereby increasing the likelihood that it is a cloud.

The test is designed primarily to detect clouds that are obviously cold, i.e., that have low physical temperatures and therefore high bases and tops. If the observed brightness temperature value is lower than the threshold then the pixel is classified as cloud filled. Over both land and water backgrounds the TIR1 thermal IR-channel brightness temperature is compared to the empirically assigned clear/cloud threshold value obtained from a corresponding Polar-Region threshold database.

However, infrared data often contain confounding cloud information over the polar ice caps during the long polar-winter night, potentially making any single-channel cloudy-pixel decisions less reliable in these regions. This is because extreme radiational cooling often drops background snow and ice temperatures to values at and even lower than any atmospheric troposphere temperatures. Locations where this effect is most dramatic are the polar mountain regions where little or none of the surface-radiated energy is trapped by the altitude-thin atmosphere before it reaches space. Targeted locations include the Greenland snowcap and the interior mountain ranges of Antarctica. Figure 4 shows

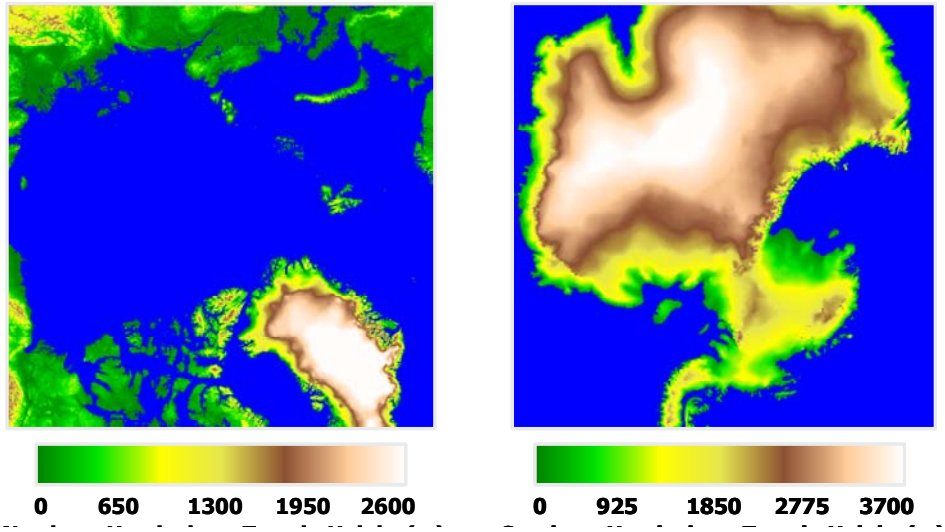

Figure 4. Maps of terrain height (meters) for the north (left) and south poles (right) – note the different scales.

terrain heights at each pole. Locations with elevations higher than ~2000 m have the greatest potential for generating clear-scene TIR brightness temperatures at and below 225 K during the polar night.

Because polar backgrounds of ice and snow provide challenging backgrounds for single-channel TIR cloud-detection tests (since they too can be quite cold), the obvious-cold test mitigates false-cloud detection over snow and ice in two ways: (1) in the polar night, when radiational cooling can be so extreme as to generate surface skin temperatures at or below even atmospheric tropopause values, terrain height coupled with a time-of-year (i.e., season-identifying) metric is used as a predictor of strong radiational cooling; (2) during daytime, results of the 1.6-μm SWIR snow/ice-detection test will obviate the results of the obvious-cold test. However this step is not performed until the cloud-mask/phase portion of the algorithm is invoked.

5 Nighttime Fog/Stratus Cloud Test for Polar Backgrounds

The low-cloud and fog test for non-solar-illuminated scenes exploits the fact that during nighttime conditions the observed 3.7-μm brightness temperatures are comprised solely of an emitted-energy component. As will be described shortly, even twilight amounts of reflected-solar energy confound the multispectral 3.7/11-μm fog signal. The primary cloud discriminator is the magnitude of the TIR-MWIR brightness-temperature difference, which, for most water-droplet clouds, is a strong and unambiguous indicator of cloud phase. The lower the MWIR temperature is from the TIR, the higher the likelihood that the pixel is filled with a water-droplet cloud.

This test is designed primarily to detect water-droplet clouds, including those in an inversion boundary layer. Water droplets have a low imaginary refractive index at 3.7 μm; in fact, it is roughly an order of magnitude lower than that at 10.8-μm TIR wavelengths. Subsequently, radiative physics dictates that the bulk emissivity of a water-droplet cloud will be lower at the shorter MWIR wavelengths. Conversely the TIR imaginary refractive indices are so high that most water-droplet clouds radiate as blackbodies with emissivity ≈ 1. The net result is that lower MWIR emissivity manifests itself as a lower observed brightness temperature in comparison to its TIR counterpart. The fog/stratus test exploits these facts by comparing the 10.8-μm TIR1 brightness temperature to the 3.7-μm MWIR value. If the 3.7-μm value is lower than the 11-μm value by an amount greater than a tunable polar-cloud detection threshold then the pixel is classified as cloud-filled. Figure 5 shows a sample image with nighttime low clouds over the South Pole.

Because the MWIR water-droplet cloud reflectivity is nontrivial, care must be taken to ensure that no incoming MWIR energy at cloud top is available for reflection. This condition restricts use of this fog/stratus test to nighttime, since the sun provides a substantial source of incoming top-of-cloud energy during daylight hours. As a consequence the daytime TIR-MWIR spectral signatures are such that the

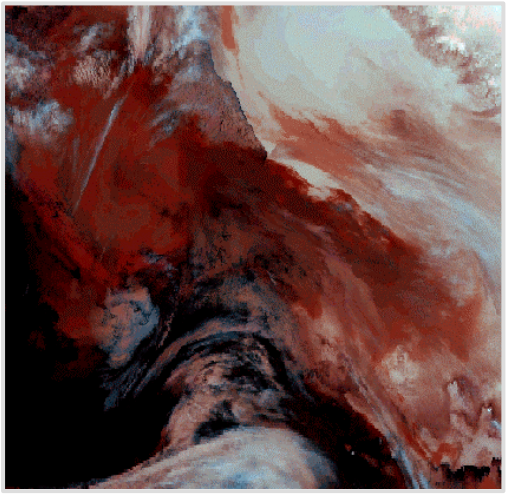

Figure 5. Nighttime boundary-layer fog and stratus appear as reddish pixels in this Antarctic-winter MWIR/TIR color composite. The strong contrast between the red and adjacent pixels provides a visual cue as to the robustness of the nighttime fog/stratus test

MWIR brightness temperatures, comprised of both emitted and thermal components, exceed the TIR temperatures by upwards of 20 K and more. For this reason a check on the scene solar elevation angle is performed to ensure that nighttime conditions are present before the test is executed.

It is useful to note, however, that this check may have minimal influence since the MWIR data are replaced by SWIR data in the daytime on some TIROS satellites carrying the AVHRR-3 instrument. Switching is performed onboard the satellite on a scene-solar-elevation basis. Thus in some cases little

MWIR data are available in daytime viewing conditions.

Sometimes a positive nighttime TIR-MWIR signal is observed over cloud-free polar ice caps because sensor noise is high in the 3.7-μm band. Thus it is important to minimize this test's detecting any pixels that (a) exhibit this signature, and (b) that are not actually clouds but rather clear-column pixels observed under conditions of extreme radiational cooling. The fog/stratus test employs two checks to minimize false detection of clouds. The first is to check on the absolute magnitude of the TIR1 brightness temperature. In most parts of the world, cloud-condensation nuclei (CCN) aid in droplet formation at relatively high atmospheric temperatures. In the non-oceanic Arctic and Antarctic, there are generally not a lot of CCNs available to aid in cloud-droplet formation. Subsequently, super cooled water droplets are common and exist at temperatures indicative of ice particles in mid-latitudes and the tropics. Consequently the nighttime fog/stratus test will flag pixels as containing water-droplet clouds down to TIR brightness temperatures at or above a certain super cooled threshold, as defined in the polar-cloud threshold table. It is common for super cooled water droplets to exist at temperatures as low as 238 K; we do not often find evidence of water droplets at lower temperatures in AVHRR polar imagery.

The second check is to isolate the use of this test inside regions of extreme radiational cooling wherein background snow and ice temperatures drop to values at and even lower than any atmospheric troposphere temperatures. Locations where this effect is most dramatic are the mountainous regions where little or none of the surface-radiated energy is trapped by the altitude-thin atmosphere before it reaches space. Targeted locations include the Greenland snowcap and the interior mountain ranges of Antarctica. Figure 4 shows terrain heights at each pole. The fog/stratus test is not applied over high-terrain regions, as defined by the polar-threshold terrain height value.

6 Nighttime Thin Cirrus Cloud Test for Polar Backgrounds

The nighttime cirrus test for non-solar-illuminated scenes exploits the wavelength-differential dependence of the Planck function on temperature. Its success is based on the seemingly peculiar (but very handy) characteristics of how objects emit electromagnetic energy at differing wavelengths. At 10.8-μm TIR1 wavelengths, blackbody radiance is somewhat linear with temperature at all commonly observed tropospheric temperatures. At 3.7 μm, however, the relationship between radiance and temperature is highly nonlinear. The differences are such that a small increase in MWIR radiance is representative of a larger increase in an object's

emission temperature, when compared to a similar (proportionate) increase in the TIR. This of course has absolutely no bearing on the consequences of observing a perfect blackbody at both wavelengths: in such a case, the MWIR and TIR brightness temperatures would be the same, regardless of the increased sensitivity of the MWIR radiance to temperature.

An example of a cloud that does not behave like a blackbody is an optically thin cirrus cloud. In such a case the cold cirrus is emitting some energy spaceward, but is also allowing some energy emitted from warmer backgrounds below to pass on through without any interaction with the ice particles. Under such conditions the satellite-observed MWIR and TIR radiances will be some combination of lower radiant energies from the cold cirrus cloud and higher energies from the warmer underlying background. In such a case the observed brightness temperature is representative neither of the true physical temperature of the background nor of the cloud, but rather of someplace in between. However, the increased sensitivity of 3.7-μm radiances to the warmer part of the scene means that the MWIR brightness temperature will be closer to the higher background temperature than its TIR counterpart. This results in a positive MWIR-TIR1 brightness temperature difference.

Take for example a pixel filled with a cirrus cloud with a physical temperature is 230 K, an emissivity is 0.5, and that lies over a warm background at 280 K. Because of the increased sensitivity of the MWIR to higher temperatures, only 5% of the satellite-observed MWIR radiance originates from the cirrus itself; in the TIR, 26% comes from the cirrus. With these figures it is easy to see that the MWIR brightness temperature will be weighted closer toward the warmer background: the MWIR brightness temperature works out to be 267.3 K, while the TIR is 258.9 K. There are other second-order radiative effects of ice particles and the atmosphere that augment this cirrus signature, but the Planck differential temperature dependence is by far the strongest. The nighttime infrared color composite in Figure 6 illustrates the robustness of this signal.

The nighttime cirrus cloud test for non-solar-illuminated data makes a cloud decision by comparing the AVHRR MWIR channel 3b value to that of TIR1 channel 4. If the 3.7-μm value is greater than the 10.8-μm value by an amount defined by a cloud detection threshold then the pixel is classified as cloud-filled.

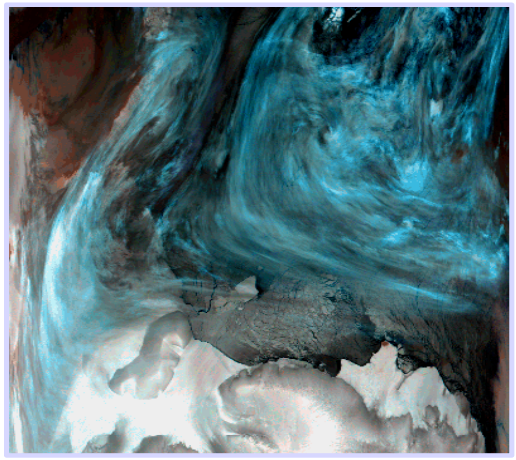

Figure 6. Nighttime cirrus appear as bluish pixels in this Antarctic-winter MWIR/TIR color composite. The strong contrast between the blue and adjacent pixels provides a visual cue as to the strength of the nighttime cirrus test

In mid latitudes and the tropics, empirical study has found in regions of high humidity that this test can over-analyze cloud. It is conjectured that large amounts of water vapor near the surface preferentially attenuate the 10.8-μm signal by several Kelvins, thereby decreasing the strength of the thin-cirrus signal. However in polar regions the atmosphere is generally quite dry. There has been no evidence to date that suggests the thin-cirrus cloud detection results are being adversely influenced by high amounts of water vapor. Hence, unlike the CDFS mid-latitude and tropical algorithms, there is no adjustment of the polar thresholds or channels that are dependent on water-vapor amounts.

Sometimes the positive nighttime MWIR-TIR signal is observed falsely over the extremely cold polar ice caps because sensor noise is so high in the MWIR band. This test has a check to isolate its use inside regions of extreme radiational cooling wherein background snow and ice temperatures drop to values at and even lower than any atmospheric troposphere temperatures. Locations where this effect is most dramatic are the mountainous regions where little or none of the surface-radiated energy is trapped by the altitude-thin atmosphere before it reaches space. Targeted locations include the Greenland snowcap and the interior mountain ranges of Antarctica. Figure 4 shows terrain heights at each pole. The nighttime thin cirrus test is not applied over high-terrain regions, as defined by the polar-threshold terrain height value.

7 Split Long-Wave Infrared Cloud Test for Polar Backgrounds

The long-wave IR cloud test compares the split-window TIR1-TIR2 brightness-temperature differences to an empirically defined split-TIR threshold. Pixels with split-TIR brightness-temperature differences at or higher than this threshold are always considered cloud-filled. This test predominantly flags cirrus-filled pixels as cloudy, although it can pick up low-cloud edges if the threshold is set too low.

The split longwave infrared test exploits the fact that TIR1-TIR2 brightness temperature differences exhibit a small but very persistent signature in this spectral region. There are three radiative effects that combine to account for the split-LWIR cirrus signatures. First, ice-particle (and to a somewhat lesser extent, water-droplet) emissivity is higher at 12 μm than at 10.8 μm. Second, atmospheric water vapor attenuation is generally stronger at the longer 12 μm wavelengths. In the poles though, this effect is minimal since polar atmospheres tend to be very dry. Third, there is a slightly stronger Planck dependence on temperature at the shorter 11-μm wavelengths, resulting in a higher 10.8-μm brightness temperature for what are essentially mixed fields of view that occur with transmissive cirrus. This is precisely the same effect as that described in Section 6, albeit much weaker. Each factor contributes to cirrus brightness temperatures that are consistently higher at 10.8 μm than at 12 μm.

The first factor is predominantly responsible for the noted persistence of the positive TIR1-TIR2 cloud signature in the Arctic. The reason is due to another obscure but fascinating phenomenon of ice-particle radiative-transfer physics in the long-wave spectrum, called tunneling. There are three ways in which a traveling TIR photon can interact with cirrus ice particles. The first is that the photon is blocked by the ice particle simply by virtue of its having encountered the particle's geometric cross section. The second is one of edge trapping wherein incident light waves skim the edge of the particle and are bent inward. There they can stay trapped along the particle edge or reflect continuously off the inside edges of the particle for long periods of time. These effects are equally strong at 10.8 and 12 μm. The third process describes how waves outside the particle's geometric cross section are still influenced by surface-wave interactions that occur closer to the ice-particle surface. This effect is much stronger at 12 μm (TIR2) than it is at 10.8 μm, resulting in TIR2 cirrus emissivities that are consistently larger than their TIR1 counterparts. In the presence of optically thin cirrus with small, nearly spherically shaped particles, this means more of the upwelling energy at 12 μm originates from the colder cloud than at 10.8 μm. The net result is that the TIR2 brightness temperature is lower than the TIR1 temperature, and their TIR1-TIR2 difference is positive.

In the tropics and mid-latitudes, and in the absence of cloud, water vapor attenuation can by itself cause a positive TIR brightness temperature difference that could be mistaken for a cloud signature. In non-polar regions the CDFS algorithm employs TIR1-TIR2 cloud-detection thresholds that are a function of water vapor along the atmospheric path. However in Polar Regions the atmosphere is so dry and clean that the need for a water-

vapor-dependent threshold is obviated.

The split-TIR cloud test makes a cloud decision by comparing the AVHRR TIR1-TIR2 brightness temperature difference to a tunable threshold. If the 10.8-μm value is greater than the 12-μm value by an amount greater than the cloud detection threshold then the pixel is classified as cloud-filled. The test works both day and night, and is independent of the scene illumination and viewing geometries. A sample mask is contained in Figure 7, near Novaya Zemlya in northwest Siberia.

Sometimes a false TIR1-TIR2 cloud signal is observed over cloud-free but extremely cold polar ice surfaces during the polar winter night. It is currently thought that sensor noise is to blame, although the precise reasons are not entirely clear. However false masks are obvious: a false TIR1-TIR2 cloud mask takes on the general shape of terrain features in the Antarctic mountains and over the interior Greenland snowcap. Thus this test has restricted use in regions of extreme radiational cooling – namely high-terrain near-polar locations during the winter night. At night, only pixels with a terrain height below a tunable threshold value are subjected to this test. Once the sun has risen to a high enough elevation, mixing near the surface eliminates this effect. During daytime when the sun is high enough in the sky (as defined by a solar zenith angle threshold), the test is used whenever TIR1 and TIR2 data are available.

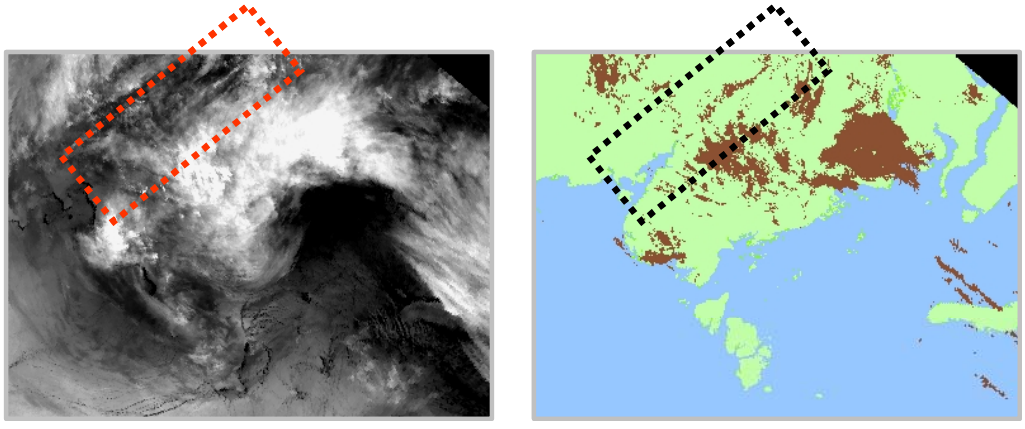

Figure 7. TIR1 image (left) and associated split-TIR-window cloud mask (right) for a cirrus scene over the north pole. The dotted rectangles are placed for reference purposes. Note that cirrus clouds are predominantly flagged by this test.

8 MWIR-TIR Daytime Cloud Test for Polar Backgrounds

The MWIR-TIR cloud test for solar-illuminated scenes compares MWIR-TIR1 brightness-temperature differences to an empirically defined threshold from the polar-cloud threshold table. Pixels with brightness-temperature differences at or higher than this threshold are always considered cloud-filled. This test flags both low- and high-cloud pixels.

The MWIR-TIR solar-illuminated data test relies on the radiative characteristics of water-droplet and ice-particle clouds at 3.7 μm. As discussed in Sections 5 and 6, both water and ice clouds have MWIR emissivities less than one. For both cloud types conservation of energy prescribes that their reflectivities are non-zero: for cirrus, the non-emissive characteristics of the clouds are manifest as a combination of transmissivity and reflectivity; for fog and stratus, it is mostly reflectivity once the optical thicknesses are large. Although low clouds tend to be more efficient reflectors of MWIR energy, each cloud type reflects MWIR data spaceward both day and night. During the night there is little downwelling MWIR radiant energy available for reflection; what little there is reaches cloud top having been generated by a cold and poorly emitting atmosphere. Thus at night the MWIR brightness temperatures are not dominated by a strong reflected component even though the actual cloud reflectivity may be substantial. There is simply a lack of 3.7-μm downwelling radiant energy available at cloud top for upward reflection back to space.

However, the instant a cloud scene becomes even tangentially illuminated by the sun, there is quickly available incident solar energy in the MWIR band that is reflected back to space. Even if the cloud reflectivity is small, incoming solar energy is so large (even at low sun angles) that the product of the two adds a significant contribution to the emitted-only portion of the upwelling radiance. Even before the sun reaches the local horizon, cirrus clouds are illuminated from below and forward-scatter that energy spaceward. The net result is that the cloudy MWIR brightness temperatures increase with increasing amounts of solar input; as the sun rises in the sky from below the horizon, clouds appear hotter and hotter at 3.7 μm, often by 6-10 Kelvins or more just a few minutes after sunrise. Meanwhile the 11-μm TIR brightness temperature is essentially unaffected by the presence of the sun – changes in TIR brightness temperatures caused by the addition of reflected sunlight are negligible.

During solar-illuminated conditions, the measured MWIR channel 3b radiance is therefore a combination of both emitted and reflected energy. At the longer channel 4 TIR wavelengths there is only an emitted component. The net result is that the MWIR brightness

Figure 8. MWIR-TIR1 image (left), the associated daytime MWIR-TIR cloud mask (center), and the corresponding visible image (right) for a cirrus scene over northeast Siberia and the north pole. Both low and high clouds have MWIR emissivities less than one; their reflectivity values yield higher brightness temperatures at 3.7 μm than at 10.8 μm for even the slightest amounts of solar illumination. The result is a cyan appearance of the cloudy pixels in the vicinity of the terminator in the MWIR-TIR composite. The hard line in the left and center images (running from upper left to lower right) is the AVHRR channel3b/3a switch point

temperatures that are representative of cloud are much larger than those for the TIR, while for other surfaces they are more nearly the same. The cloud test is applied by comparing the MWIR - TIR brightness temperature difference. The test assumes that liquid water and thin cirrus clouds will reflect enough solar energy at 3.7 μm to make the channel 3b brightness temperature significantly higher than the brightness temperature at channel 4. If the channel MWIR brightness temperature is greater than the TIR1 value by an amount greater than a tunable cloud detection threshold the pixel is classified as cloud-filled.

This test is of only limited usefulness when the AVHRR-3 is programmed to transmit channel 3a during daytime, since that results in the loss of the MWIR channel. Figure 8 shows how abruptly and close to the terminator the channel switching occurs on NOAA-17. Nonetheless the daytime MWIR-TIR difference test has value in that it is a robust indicator of cloud; additionally, not all AVHRR-3 sensors are programmed for near-IR/SWIR channel switching.

Sometimes the positive MWIR-TIR1 cloud signal is observed falsely over the extremely cold polar ice caps in the polar winter terminator. It is currently thought that high sensor noise in the 3.7-μm band is to blame. Thus this test has restricted use in regions of extreme radiational cooling – namely high-terrain locations in the long winter night. This test is applied only to pixels where the terrain height is below a tunable threshold value.

9 Mosaic Databases Required for Temporal Differencing Cloud Tests

As will be discussed in the next 3 sections, temporal differencing tests are used to analyze Polar Region data. These are analogous to the temporal differencing tests currently used in CDFS-II to analyze geostationary data (see d'Entremont and Gustafson, 2003), with the major difference being that it is applied to polar-orbiting data. Because of the large overlap between consecutive orbits, and the temporal stability of polar backgrounds (relative to the diurnal changes in mid latitudes and tropics), it is possible to apply similar techniques to the polar orbiting data at high latitudes. To accommodate the shift in sub track with each orbit it is necessary to put all the data from current and previous orbits into a common projection. A polar-stereographic projection similar to the AFWA grid was selected, however, to minimize distortion it is defined with a true latitude of 80° and a resolution of 4 km.

After each orbit from a given satellite is processed, a post processing step extracts all data poleward of 70° latitude and maps it into the new polar grid – one each for the North and South polar regions (Figure 9) – with newer data overwriting older. In this way a mosaic database is established that contains the most recent data available from the satellite. This in turn is used as a baseline to identify locations in any new data where there has been a recent change. Each polar grid database contains separate mosaics of the midwave and thermal IR channel data, valid time, and solar zenith angle.

The process of co-registering the satellite data to the polar stereographic grid has the additional benefit of minimizing the amount of over- and under-sampling that occurs with AVHRR GAC pixels (nominal 4-km resolution) during the transformation process. Mapping accuracies must be to within one pixel. Any registration errors that exist between two or more images can result in false cloud signatures. For example, along an ice edge, a water pixel in one image may be misaligned to an ice pixel in the next image. Since it is likely that the TIR brightness temperatures measured from the two different backgrounds will differ significantly, the temporal difference algorithm is likely to misclassify the pixel in at least one of the scenes as cloud-filled.

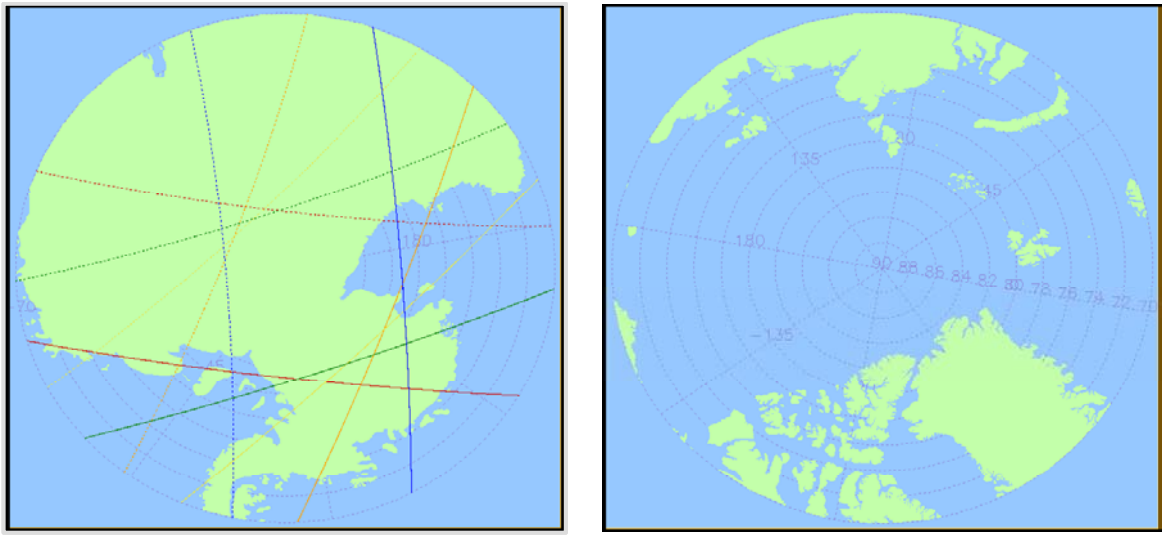

Figure 9. Southern and Northern polar grids used for the temporal differencing mosaic files. The Southern grid has superimposed sub tracks for several consecutive NOAA-17 orbits

10 Thermal Infrared Temporal Differencing Cloud Test for Polar Backgrounds

The thermal infrared temporal difference test identifies new cloud development and existing cloud features in polar scenes that have moved over either previously clear background or lower, warmer cloud. The test exploits the change in infrared brightness temperature in the 10.8-μm TIR1 channel, on a pixel-by-pixel basis, caused by both moving and developing cloud features in collocated pixels taken from time-sequential polar satellite images. TIR1 data from the current satellite pass are compared to the corresponding data maintained in the Polar Mosaic database described in Section 9. The test requires that the satellite-observed brightness temperature decrease over time by an amount greater than an empirically defined threshold in order for the analysis pixel to be flagged as cloud-filled. The infrared temporal difference test is executed at all times day and night.

Since this test keys on changes in brightness temperature between two co-located pixels to identify cloud-filled pixels it is important to recognize that some differences will occur even for cloud-free pixels. In mid-latitudes and the tropics the current CDFS temporal differencing algorithms used with geostationary satellite data (see d'Entremont and Gustafson, 2003) require knowledge of the time rate-of-change of the satellite observed infrared brightness temperature for the clear-scene background. In Polar Regions diurnal temperature changes tend to be much smaller. However, since there are no reliable estimates of clear-scene brightness temperatures

available the polar temporal-differencing cloud detection thresholds must be set somewhat conservatively (i.e., some clouds may be missed) before clouds are flagged.

The change in satellite-measured brightness temperature is computed as follows:

$$\Delta T_{TIR} = T_{TIR}(t) - T_{TIR}(t-\Delta t),$$

where $T_{TIR}(t)$ represents the brightness temperature for the TIR1 sensor channel measured at the current observation time, and $T_{TIR}(t-\Delta t)$ represents the brightness temperature at the corresponding location in the mosaic database. The measured brightness temperature difference ΔT_{11} is compared to a tunable threshold to determine if cloud has either formed within or moved into the pixel FOV during the intervening time period Δt. If ΔT_{11} is greater than a prescribed temperature-difference threshold, boundary-layer inversion fog may exist in that pixel. Figure 10 shows an example of the IR temporal differencing test results.

Polar-orbiting satellites do not view the same area of the poles during each scan, although there are regions closely adjacent to each pole that are viewed during every overpass. This routinely results in a different time difference Δt between new and previous pixels over different parts of a polar scene. Therefore, valid times are checked for each pixel to insure that a correct Δt is within acceptable limits (as defined by the polar-threshold table) before temporal differencing tests are applied.

Once the single-channel TIR temporal difference test has identified new boundary-layer clouds, information can be obtained on their thermal structure within a local region. Since the thermal structure of cloud features will vary significantly over any image scene, a single scene-average cloud temperature will not provide information accurate enough to define useful cloud thresholds throughout the entire image. Therefore, the scene is first divided into user-defined analysis boxes and dynamic cloud thresholds are established for each box individually. The minimum and maximum brightness temperatures of the cloud-filled pixels from temporal differencing are identified and used to define a local infrared brightness temperature cloud threshold.

The cloud threshold T_{cloud} is defined as:

$$T_{cloud} = \gamma T_{min} + (1 - \gamma) T_{max},$$

where γ is a tunable factor used to eliminate anomalous warm pixels from the threshold calculation, and T_{max} and T_{min} are the maximum and minimum brightness temperatures, respectively, of the pixels classified as cloud-filled by the temporal difference test within the image analysis box. High γ values mean more dynamic thresholding; low

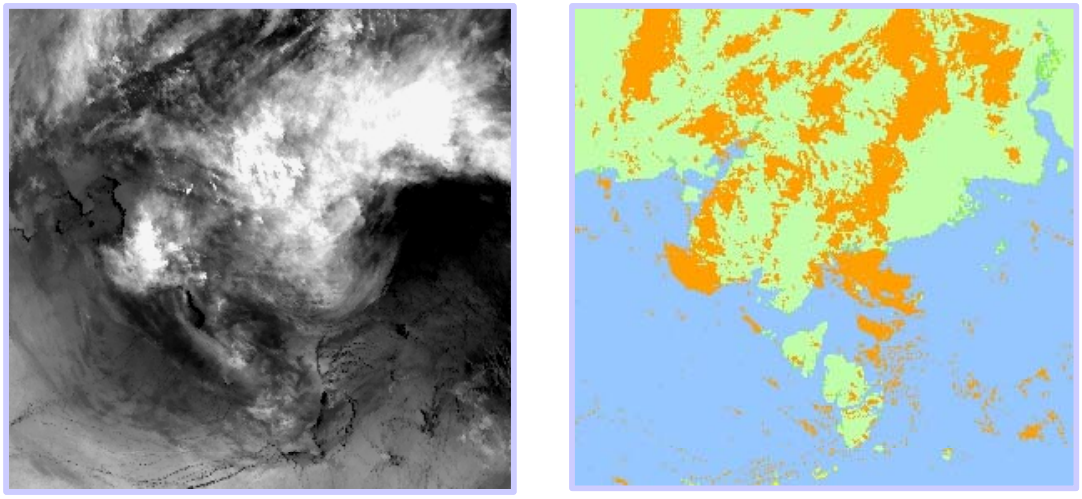

Figure 10. TIR1 image (left), and the associated TIR temporal differencing cloud mask (right) for a scene over northern Siberia. The cloud system is moving westward (right to left): note how the leading edges of the advancing clouds are picked up by the temporal differencing test.

values mean less. The dynamic-threshold test is only performed when the total number of in the analysis box classified as cloud-filled by temporal differencing exceeds a defined threshold, which is expressed as a tunable percentage of the total number of pixels in that analysis box. This check is performed to minimize any noisy or misaligned satellite data from adversely affecting the dynamic threshold cloud detection process. If the percentage criteria are met all pixels in the local analysis box are evaluated: if TIR1 $\leq T_{cloud}$, the pixel is classified as cloud. Additionally, users have the option of shutting off the dynamic-threshold portion of the test by specifying $\gamma < 0$.

The dynamic threshold test is precisely analogous to that performed in the geostationary temporal differencing tests currently run on CDFS (see d'Entremont and Gustafson, 2003). This process is illustrated in Figure 11.

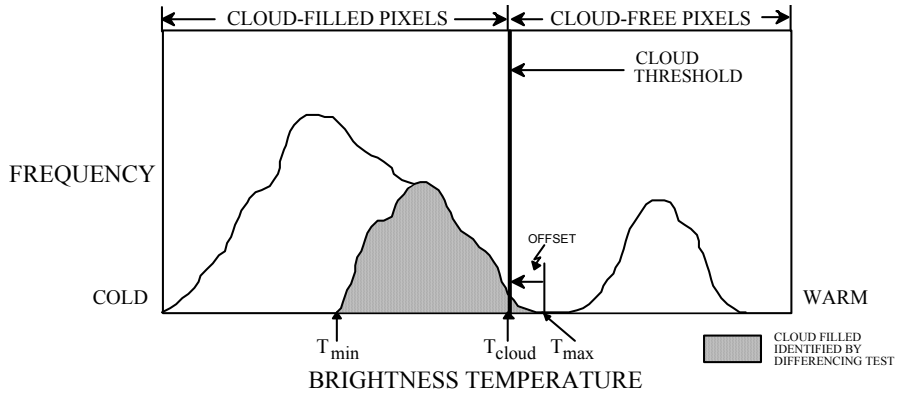

Figure 11. Conceptual approach to the dynamic threshold technique for pixels within a local analysis box

11 Nighttime Fog Temporal Differencing Cloud Test for Polar Backgrounds

The night fog temporal difference (TD) test identifies new fog development and advection of pre-existing fog/low-stratus features in polar scenes that have formed within a strong polar boundary-layer inversion. Like the single-channel TIR temporal differencing technique outlined in Section 10, this test also exploits the change in infrared brightness temperature in the 10.8-μm TIR1 channel, on a pixel-by-pixel basis, caused by both moving and developing fog in collocated pixels taken from time-sequential polar satellite images. The difference between the two tests, however, is that the fog TD test identifies *warming* (as opposed to cooling) temporal signatures. This is because fog in the polar inversion is warmer than the underlying snow/ice surface during the polar night (this difference can often be several 10's of K). When fog either advances into or forms within a surface inversion over a very cold background, the TIR1 brightness temperature rises dramatically, and from that temporal signature the presence of boundary-layer inversion stratus can be inferred with some confidence. This test is performed only at night.

TIR1 data from the current satellite pass are compared to the corresponding data maintained in the Polar Mosaic database described in Section 9. The test requires that the satellite-observed brightness temperature *increase* over time by an amount greater than an empirically defined threshold in order for the analysis pixel to be flagged as cloud-filled. The change in satellite-measured brightness temperature is computed as in Section 10. If ΔT_{TIR} is greater than a prescribed temperature-difference threshold, then boundary-layer inversion fog may exist in that pixel.

To ensure the warming is due to clouds and not a background change, a final spectral test is performed. The warming temporal-difference pixels must also exhibit a

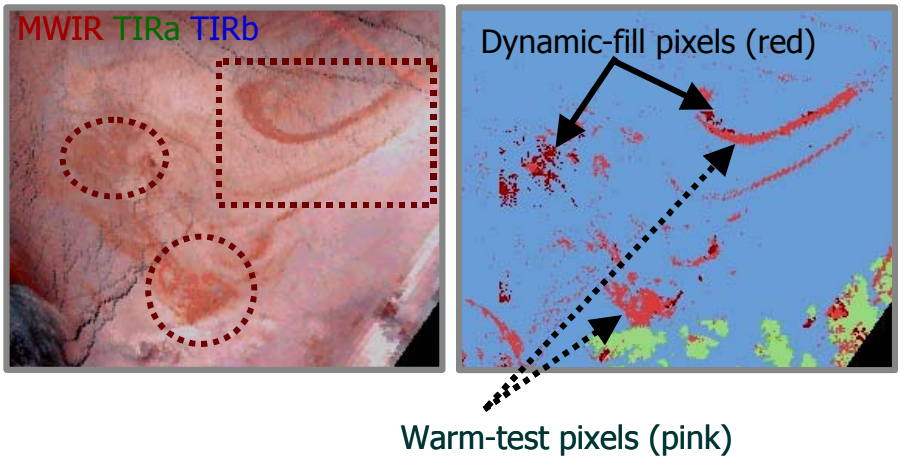

Figure 12. MWIR-TIR color composite image (left) and associated night fog temporal differencing cloud mask (right) for a cirrus scene over the north pole. The dotted rectangles are placed for reference purposes. Note that inversion-layer low clouds and fog appear reddish in the color composite.

positive TIR1-MWIR spectral difference as well, as suggested by the discussions in Section 5, before a pixel is finally classified as cloud-filled by the MWIR-TIR fog/stratus temporal differencing test. The MWIR-TIR infrared temporal difference test is executed only at night, in search of inversion fogs.

Once the single-channel TIR temporal difference test has identified new boundary-layer clouds, a dynamic threshold is computed as described in Section 10. If the percentage of cloudy pixels detected by temporal differencing criteria are met all pixels in the local analysis box are evaluated: if TIR1 $\geq$ T_{cloud} , the pixel is classified as cloud. As described above, users have the option of shutting off the fog dynamic-threshold portion of this test by specifying $\gamma < 0$.

Sometimes this test may flag warmer open-ocean regions among moving ice floes as fog. In order to minimize the false detection of inversion fogs under such conditions, a final check is performed on the absolute magnitude of the TIR1 brightness temperature. If the TIR1 temperature is greater than an empirically defined sea-ice/water temperature threshold (based on the freezing point of sea water), the fog-stratus temporal difference test does not detect cloud. Figure 12 provides an example of results from the Night Fog Temporal Differencing Test, with dynamic thresholding enabled.

12 Summary Remarks

Cloud determination of an AVHRR analysis pixel is based on the evaluation of results from the individual cloud tests. In polar regions, as defined by tunable latitude thresholds, the new tests

described in Sections 2 - 11 are applied. In general, if any of the nighttime tests detect cloud then the pixel is classified as cloudy; during daytime conditions additional checks are performed to avoid misinterpretation of highly reflective snow/ice backgrounds as cloud. Individual tests have applicability criteria: for purposes of the final cloud classification any test that was not run due to failure to meet these criteria are treated as if they produced a negative result. For example, the Near-Infrared Brightness Cloud Test (Section 3) is not allowed to pass over locations identified as snow- or ice-covered. Thus when evaluating the obvious-bright test result in the presence of snow, it is treated as though that test did not detect cloud.

On a final note, the spectral characteristics of mid-latitude and tropical backgrounds are relatively well behaved in that the existing AFWA CDFS algorithms have predictive skill in characterizing their radiative and spectral nature. There are several reasons for this. First, daytime solar elevation angles are high enough so that scenes are well illuminated by the sun during daylight observations. Second, analyses from non-satellite sources (such as surface skin temperature and NWP models) have enough skill to be useful to the cloud tests in defining many background attributes.

However in polar regions, scenes are typically not well sunlit during daytime. Even when solar elevations are high, snow and ice are easy to confuse with clouds. Polar nights can be long and radiative cooling of snow and ice backgrounds can be so extreme that numerical models have little or no background predictive skill. Thus the set of polar cloud-detection tests (Sections 2-11) have been designed to require no support from non-static background databases.

13 References

d'Entremont, R. P., and G. B. Gustafson, 2003: Analysis of Geostationary Satellite Imagery Using a Temporal-Differencing Technique. Earth Interactions, **7**, Paper 1.

Liu, Y., J. Key, R. Frey, S. Ackerman, and W.P. Menzel, 2004: Nighttime polar cloud detection with MODIS, *J. Appl. Meteorol.*, **92**, 181-194.

Shi, T., Yu, B., Clothiaux, E. E., and Braverman, A. J., 2004: Improving Polar Cloud Detection by fusing MISR and MODIS data. (http://www.stat.ohio-state.edu/~taoshi/research.html)

Spangenburg, D. A., D. R. Doelling, V. Chakrapani, P. Minnis, and T. Uttal, 2002: Nighttime cloud detection over the arctic using AVHRR data. Twelfth ARM Science Team Meeting Proceedings, St. Petersburg, Florida, 8-12 Apr 2002.